Appl Phys A (2013) 112:263–267
DOI 10.1007/s00339-013-7744-x

Applied Physics A
Materials Science & Processing

RAPID COMMUNICATION

Microstrip notch filters based on open interconnected split ring resonators (OISRRs)

Juan de Dios Ruiz · Juan Hinojosa · Alejandro Alvarez-Melcon

Received: 18 March 2013 / Accepted: 30 April 2013 / Published online: 8 May 2013

Abstract An open interconnected split ring resonator (OISRR) is proposed for use in compact microstrip notch filters. This OISRR behaves as a shunt series $L\,C$ resonant circuit and allows a parallel connection with a microstrip line. This cell presents half the resonant frequency of the split ring resonator (SRR) and, therefore, is electrically very small. The measured results show a 3 dB stop-band bandwidth lower than 2 % with more than 10 dB insertion loss in the stop band. This OISRR can be useful in microwave communication systems.

1 Introduction

Microstrip band-stop filters (BSFs) find many applications in microwave systems to filter in desired signals and to reject unwanted signals. However, the BSFs have not been extensively investigated in comparison with their band-pass and low-pass counterparts. The conventional techniques to implement BSFs use shunt stubs or stepped-impedance microstrip lines [1]. These filters have a narrow stop-band response and a large circuit size. Electromagnetic band gap (EBG) structures and defected ground structures (DGSs) can be a solution to increase the stop-band bandwidth [2–4]. However, these filters require several cells of a periodic structure to provide a significant level of stop-band rejection and, therefore, can be relatively large to operate at certain frequencies. To reduce filter size, slow-wave open-loop resonator structures and metamaterial-inspired structures can be used [5–7]. In these implementations, the resonators are electrically or magnetically coupled to a host line, connected either in series or in shunt configurations. The metamaterial-inspired structures are based on split ring resonators (SRRs), open split ring resonators (OSRRs) and their respective complementary counterparts [8–10].

In this paper, an open version of an interconnected split ring resonator (OISRR) is described for the novel compact design of microstrip notch filters. The basic OISRR cell behaves as a shunt series $L\,C$ resonant circuit, which allows a parallel connection with a microstrip line section. Moreover, this OISRR cell has half the electric size of the SRR cell. The structure of the microstrip OISRR-based BSF does not require tuning very small gaps (the rings are coupled inductively to a microstrip line), presents a narrow stop-band response, has higher-power capability than other existing alternatives in coplanar waveguides (CPWs) and is suitable for compact designs. The possibilities of this resonator (OISRR) are experimentally demonstrated.

2 Microstrip line loaded with an OISRR: structure, circuit model and analysis

The structure and equivalent circuit model of the microstrip line loaded with an OISRR cell are shown in Fig. 1. The basic OISRR cell (Fig. 1(a)) is conceived from two open rings of different radii. At the top side, the dimensions of the proposed structure are radius r of the external ring, width c of the ring conductors and slot s between rings. An open window $D_1 \times D_2$ is etched at the bottom side, which corresponds to the ground plane. The microstrip line width W is adjusted along the window of length D_1 in order to preserve the characteristic impedance, Z_c. As long as the size of the

J.D. Ruiz · J. Hinojosa (✉)
Department of Electronics and Computer Engineering,
Universidad Politécnica de Cartagena, 30202 Cartagena, Spain
e-mail: juan.hinojosa@upct.es

A. Alvarez-Melcon
Department of Communications and Information Technologies,
Universidad Politécnica de Cartagena, 30202 Cartagena, Spain

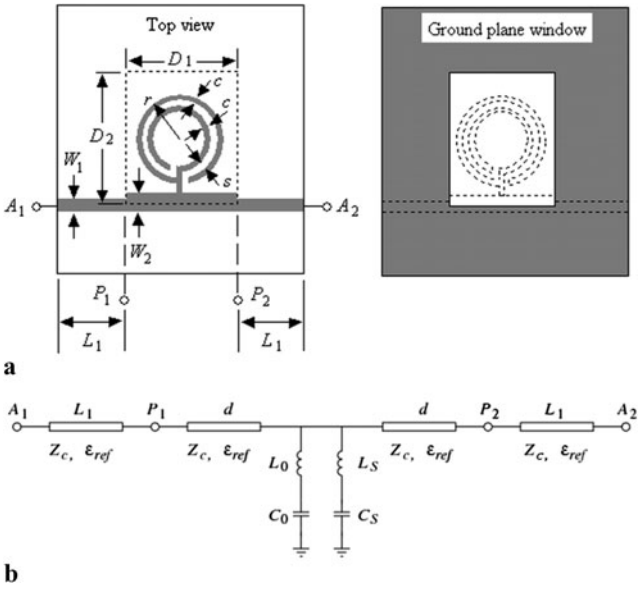

Fig. 1 Microstrip line loaded with an OISRR. (**a**) Top and bottom views and (**b**) equivalent circuit

OISRR is electrically small, the structure can be described by means of lumped elements. The OISRR structure is similar to the OSRR structure [10] with the difference that the two rings are connected to a common point of the microstrip line and, therefore, instead of having a series connection with the microstrip line, the OISRR has a parallel connection. Thus, the main resonant frequency is expected to be the same for both structures (OSRR and OISRR). Therefore, the proposed OISRR cell can be of great interest for compact designs, since it allows a small electrical size, similar to the OSRR cell.

The equivalent circuit model of the OISRR cell is shown in Fig. 1(b) (losses have been neglected in this model). It consists of two shunt series $L\,C$ resonant circuits embedded between two microstrip line sections of effective length d, which present a characteristic impedance Z_c and an effective permittivity ϵ_{ref}. The input and output ports of the structure are marked as A_1 and A_2 in Fig. 1. In view of the model, two frequencies f_0 and f_s can be identified. f_0 is the main frequency of the OISRR and is given by the resonant condition of the shunt series $L_0\,C_0$ circuit, which leads to a transmission zero (S_{21}). f_s corresponds to the spurious resonance of the OISRR cell. It is obtained by means of the shunt series $L_s\,C_s$ circuit, which also leads to a transmission zero.

$L_0\,C_0$ values are calculated from the element transformation between the OSRR and OISRR circuit models by using an impedance scaling factor α [1, 10]:

$$L_0 = \alpha\, L_{OSRR}, \tag{1}$$

$$C_0 = C_{OSRR}/\alpha, \tag{2}$$

$$\alpha = \frac{1}{4}\left(\frac{\Delta f_{OSRR}}{\Delta f_0}\right), \tag{3}$$

where L_{OSRR} is the inductance of a closed ring of averaged radius $r_0 = r - c - s/2$ and width c. C_{OSRR} is the distributed capacitance between the inner and outer rings ($C_{OSRR} = 2\pi r_0 C_{pul}$, where C_{pul} is the per unit length capacitance of the slot between the rings). L_{OSRR} and C_{OSRR} are the elements of the OSRR circuit model with substrate and dimensions identical to the OISRR cell [10]. Δf_{OSRR} and Δf_0 are the 3 dB band-pass and stop-band bandwidths at the main resonant frequencies of the OSRR and OISRR, respectively.

The shunt series $L_s\,C_s$ circuit resonates at $f_s = 1/(2\pi\sqrt{L_s\,C_s})$ and has a reactance slope $x_s = \omega_s\,L_s$. By neglecting the effect of the shunt series $L_0\,C_0$ circuit at f_s, the lumped elements $L_s\,C_s$ are derived from the transmission parameter of the two-port network (Fig. 1) terminated with 50 Ω [1]:

$$\frac{x_s}{50} = \frac{f_s}{2\Delta f_s} \quad \Rightarrow \quad L_s = \frac{50}{4\pi\,\Delta f_s}, \tag{4}$$

$$C_s = \frac{1}{L_s}\left(\frac{1}{2\pi f_s}\right)^2, \tag{5}$$

where Δf_s is the 3 dB stop-band bandwidth at the spurious resonance f_s. Finally, the effective length d of the microstrip lines in the circuit model (Fig. 1(b)) can be obtained by fitting the phase of the S_{21} parameter.

Figure 2 shows typical electromagnetic (EM) simulation and equivalent circuit results for the microstrip line loaded with an OISRR (Fig. 1). The frequency responses were obtained by using commercial simulators (ADS and HFSS). In this paper, all the structures have a copper thickness $t = 17.5$ μm and a substrate thickness $h = 0.635$ mm with a permittivity $\epsilon_r = 10.2$. The fundamental quasi-TEM mode is fed by two 50 Ω microstrip ports at the reference planes A_1 and A_2. Furthermore, all the microstrip lines have a length $L_1 = 5.5$ mm, $W_1 = 0.594$ mm and $W_2 = 0.794$ mm, which provide a characteristic impedance $Z_c = 52.3$ Ω. The element values of the shunt series $L\,C$ circuit are determined from OISRR dimensions, OSRR model [10] and EM simulation results (Fig. 2, dashed lines): $r = 2.2$ mm, $c = 0.3$ mm, $s = 0.25$ mm, $L_{OSRR} = 7.4$ nH, $C_{OSRR} = 0.8$ pF, $\Delta f_{OSRR} = 2.15$ GHz, $\Delta f_0 = 0.011$ GHz, $f_s = 4.67$ GHz and $\Delta f_s = 0.248$ GHz. Substituting the previous data into (1) to (5) and fitting the phase of the S_{21} parameter, the equivalent circuit elements (Fig. 1(b)) are extracted as follows: $\alpha = 50$, $L_0 = 370$ nH, $C_0 = 0.016$ pF, $L_s = 16.04$ nH, $C_s = 0.0722$ pF and $d = 5$ mm. As can be seen in Fig. 2, the response of the circuit model (solid lines) agrees well with the result of EM simulation (dashed lines). The microstrip OISRR-based structure presents a main frequency (first transmission zero) at $f_0 = 2.1$ GHz and a spurious resonance (second transmission zero) at $f_s = 4.67$ GHz, which is greater than twice f_0 and has a 3 dB bandwidth approximately twenty-two times greater than the

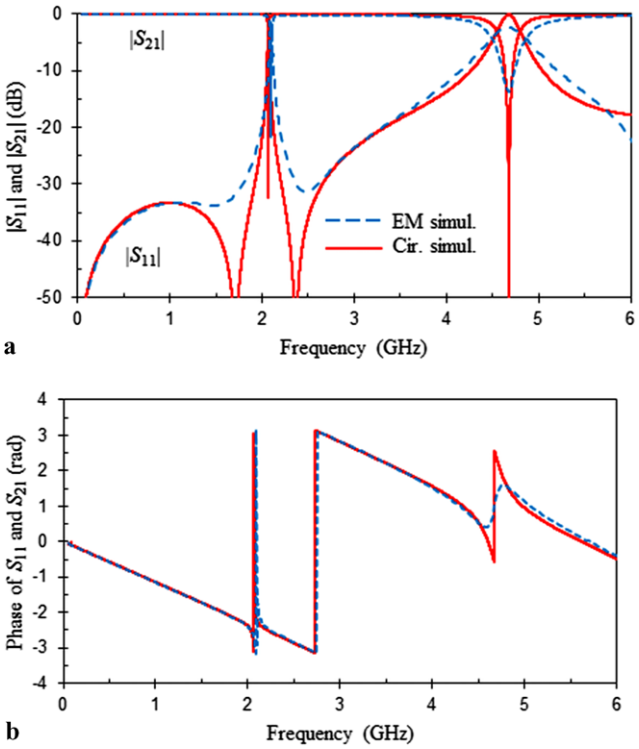

Fig. 2 EM simulation (*dashed lines*) and equivalent circuit (*solid lines*) results for the microstrip line loaded with an OISRR: (**a**) magnitude and (**b**) phase. OISRR data: $r = 2.2$ mm, $c = 0.3$ mm, $s = 0.25$ mm and $D_1 \times D_2 = 9 \times 9$ mm^2

main resonance ($\Delta f_0 = 0.011$ GHz). Moreover, two anti-resonances appear around $f_0 \pm 0.5$ GHz. The first one is due to the perfect matching condition between the ports and the microstrip OISRR-based structure, while the second one is due to the anti-resonance permittivity behavior of the OISRR [11]. The transmission zeros occur at the resonant frequencies of the OISRR, since at these frequencies there is an electric short to ground, and the injected power is reflected back to the source. The anti-resonance appears at $f_a = 2.46$ GHz because the microstrip OISRR-based structure behaves as a shunt parallel LC resonant circuit. At the main frequency $f_0 = 2.1$ GHz, this proposed OISRR works as a notch filter. At this frequency, the wavelength in the microstrip line is around $\lambda = 56$ mm ($\epsilon_{ref} = 6.4$) and the length of the filter for $D_1 = 9$ mm is below $\lambda/6$, thus confirming that the proposed design leads to compact structures.

Figure 3 illustrates the electric field distribution at four frequencies of the response of the microstrip OISRR-based structure (Fig. 2): one inside the pass band ($f_1 = 1$ GHz), two inside the two stop bands ($f_2 = 2.1$ GHz and $f_3 = 4.67$ GHz) and the last at the anti-resonance ($f_4 = 2.46$ GHz). In Fig. 3(a), we can observe that the OISRR does not resonate at $f_1 = 1$ GHz, and the signal is transmitted to the output port. Figure 3(b) shows the electric

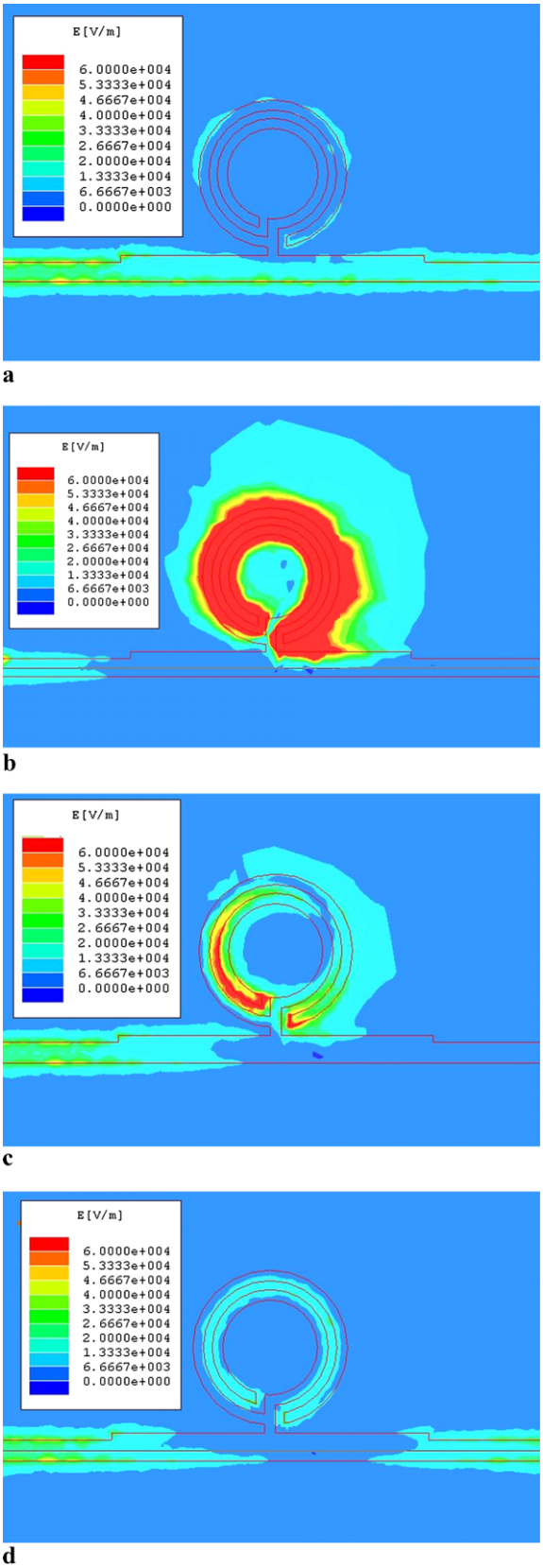

Fig. 3 Electric field distributions for the microstrip line loaded with an OISRR at the frequencies: (**a**) $f_1 = 1$ GHz, (**b**) $f_2 = 2.1$ GHz, (**c**) $f_3 = 4.67$ GHz and (**d**) $f_4 = 2.46$ GHz. OISRR data: $r = 2.2$ mm, $c = 0.3$ mm, $s = 0.25$ mm and $D_1 \times D_2 = 9 \times 9$ mm^2

field at the first stop band of the structure ($f_2 = 2.1$ GHz). We can see that the OISRR resonates at the fundamental mode, exhibiting an almost uniform field distribution. It can also be observed that the signal is reflected by this strong resonance of the OISRR, so transmission is eliminated. Figure 3(c) depicts the electric field at the second stop band of the structure ($f_3 = 4.67$ GHz), which corresponds to the spurious stop band. Again, the OISRR become resonant, but this time the electric field exhibits a zero value at the centre of the resonator, being maximum at the edges. This field distribution clearly indicates the presence of a first higher order resonant mode in the OISRR. Finally, Fig. 3(d) displays the electric field at the anti-resonance of the structure ($f_4 = 2.46$ GHz). The resonator is excited, but this time it behaves as an open circuit due to the large effective permittivity of the OISRR. At this frequency, its effective permittivity exhibits a strong resonant behavior, as studied in Ref. [11]. The OISRR acts as a magnetic wall, and the transmitted signal is mirrored to the output port.

EM and circuit simulations (Fig. 4) have been performed to study the effects of each design parameter (r, c and s) on the main resonance (f_0) and on the 3 dB stop-band bandwidth (Δf_0) of the proposed notch filter. The study will also serve to validate the equivalent circuit model. We have found that the spurious resonance appears at a frequency greater than twice the main resonance ($f_s > 2f_0$) for both circuit and EM simulations. In Fig. 4, the dashed lines show the results of the EM simulations. The main frequency (f_0) and the 3 dB stop-band bandwidth (Δf_0) decrease according to the increasing radius r of the external ring (Fig. 4(a), $c = 0.3$ mm and $s = 0.25$ mm fixed) from 2 mm to 2.4 mm. This is because the capacitance C_0, the inductance L_0 and also the reactance slope ($x_0 = \omega_0 L_0$) of the OISRR increase as r is incremented. This trend is reversed when the width c of the ring conductors (Fig. 4(b), $s = 0.25$ mm and $r = 2.2$ mm fixed) or the slot s between rings (Fig. 4(c), $c = 0.3$ mm and $r = 2.2$ mm fixed) increases between 0.1 mm and 0.5 mm. For these cases, one of the two circuit elements of the OISRR is quasi-constant, while the other decreases as c or s increases. The EM results according to the design parameters (Fig. 4) have f_0 between 1.78 GHz and 2.47 GHz, while Δf_0 varies between 0.007 GHz and 0.034 GHz. Circuit (solid lines) and EM simulation results present a reasonable agreement. The minimum and maximum relative errors for f_0 are, respectively, 0.22 % and 4.2 %, while for Δf_0 the minimum and maximum relative errors are 1.17 % and 62.4 %, respectively. The circuit model is less accurate for Δf_0 when $c > 0.35$ (Fig. 4(b)) or $s > 0.3$ (Fig. 4(c)) because of the variation of the impedance factor α, which is not taken into account in the equivalent circuit model. However, this equivalent circuit model provides a useful tool for the initial design of microstrip notch filters with the OISRR cell.

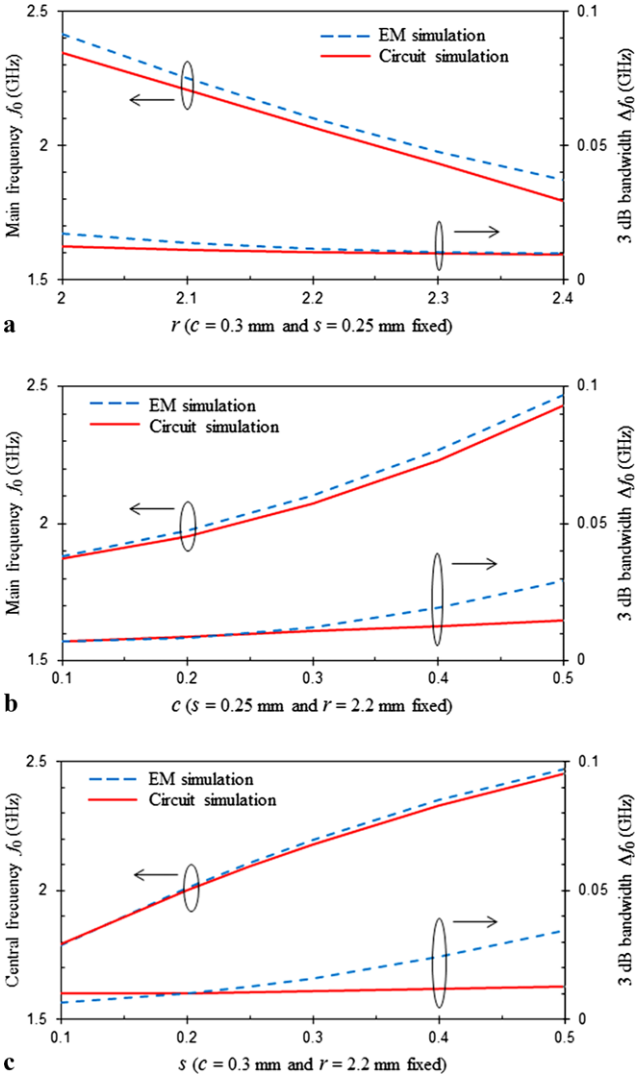

Fig. 4 Main frequency (f_0) and 3 dB stop-band bandwidth (Δf_0) for the microstrip line loaded with an OISRR according to the design parameters: (**a**) r ($c = 0.3$ mm and $s = 0.25$ mm fixed), (**b**) c ($s = 0.25$ mm and $r = 2.2$ mm fixed) and (**c**) s ($c = 0.3$ mm and $r = 2.2$ mm fixed)

3 Microstrip notch filter using OISRR

An interesting application of the OISRR can be found in the design of compact microstrip notch filters. Thus, different structures of the circuit shown in Fig. 1 have been fabricated (Fig. 5) on an Arlon AD1000 material ($\epsilon_r = 10.2$, $\mathrm{tg}\,\delta = 0.0023$ at 10 GHz, substrate thickness $h = 0.635$ mm and copper thickness $t = 17.5$ μm) and have been measured by means of a system of prototyping (LPKF protolaser S) and a vector network analyzer (Rohde & Schwarz VNA), respectively. The structures were fed with the fundamental TEM mode generated by the VNA by means of a commercial 50 Ω coaxial to microstrip transition (Anritsu 3680K test fixture). The system of measurement was calibrated from 0.01 GHz to 6 GHz. The dimensions of the

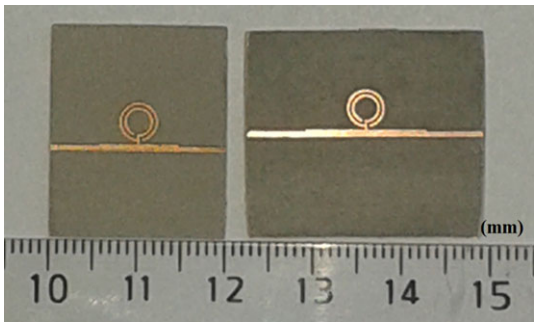

Fig. 5 Photographs of the fabricated microstrip notch filters

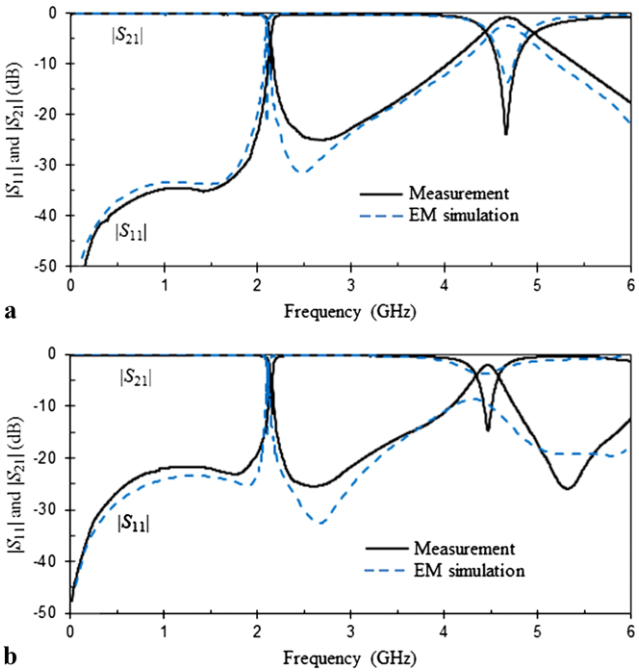

Fig. 6 EM simulation (*dashed lines*) and measured (*solid lines*) results for the microstrip line loaded with an OISRR: (**a**) $D_1 \times D_2 = 9 \times 9$ mm^2 and (**b**) $D_1 \times D_2 = 14 \times 9$ mm^2. OISRR data: $r = 2.2$ mm, $c = 0.3$ mm and $s = 0.25$ mm

OISRR cell and microstrip lines are the same as those used for the simulations shown in Fig. 2. Two different lengths D_1 of open windows were etched in the ground plane to describe its effects on the filter characteristics.

Figure 6(a) and (b) show EM simulated and measured frequency responses of the microstrip OISRR-based structures with $D_1 = 9$ mm and $D_1 = 14$ mm, respectively. As can be seen, a reasonable agreement between the EM simulation and measurement results is obtained. The microstrip OISRR-based filter with $D_1 = 9$ mm (Fig. 6(a)) has a main frequency at $f_0 = 2.14$ GHz, an anti-resonance at $f_a = 2.6$ GHz and a spurious resonance at $f_s = 4.66$ GHz, which is greater than twice the main frequency (f_0). The window D_1 only affects the spurious resonance. As D_1 is increased from two (Fig. 6(a)) to three (Fig. 6(b)) times the diameter of the external ring ($\Phi = 2r = 4.4$ mm), the spurious resonance is shifted downwards by 0.2 GHz ($f_s = 4.46$ GHz) with a slight attenuation. However, the length D_1 of the open window has little effect on the main frequency ($2.14 \leq f_0$ (GHz) ≤ 2.16), on the main 3 dB stop-band bandwidth ($1.4 \leq \Delta f_0$ (%) ≤ 1.6) and on the insertion loss in the main stop band ($11.5 \leq$ IL (dB) ≤ 12.6).

4 Conclusion

A novel compact microstrip notch filter based on an OISRR resonator has been proposed and analyzed. This OISRR is modeled as a shunt series $L\,C$ resonant circuit connected in parallel to a microstrip line. The main resonance occurs at half the resonant frequency of the SRR, increasing the compactness. The designed filter displays a 3 dB stop-band bandwidth lower than 2 % with more than 10 dB of insertion loss. Thus, this novel device is expected to be useful in microwave communication systems.

Acknowledgements This work was supported by Ministerio de Ciencia e Innovación of Spain and by FEDER (TEC2010-21520-C04-04/TCM).

References

1. J.-S. Hong, M.J. Lancaster, *Microstrip Filters for RF/Microwave Applications* (Wiley, New York, 2001)
2. J.D. Ruiz, F.L. Martínez, J. Hinojosa, IEEE Antennas Wirel. Propag. Lett. **10**, 1104 (2011)
3. D.N. Elshead, H.A. Elsadek, E.A. Abdallah, M.F. Iskander, H. Elhenawy, Appl. Phys. A **103**, 541 (2011)
4. D.J. Woo, T.K. Lee, J.W. Lee, C.S. Pyo, W.K. Choi, IEEE Trans. Microw. Theory Tech. **54**, 2840 (2006)
5. A. Vélez, G. Sisó, A. Campo, M. Durán-Sindreu, J. Bonache, F. Martín, Appl. Phys. A **103**, 911 (2011)
6. J. Naqui, M. Durán-Sindreu, F. Martín, Appl. Phys. A **109**, 1053 (2012)
7. A. Vélez, F. Aznar, M. Durán-Sindreu, J. Bonache, F. Martín, IET Microw. Antennas Propag. **4**, 712 (2010)
8. J.B. Pendry, A.J. Holden, D.J. Ribbins, W. Stewart, IEEE Trans. Microw. Theory Tech. **47**, 2075 (1999)
9. J.D. Baena, J. Bonache, F. Martín, R. Marqués Sillero, F. Falcone, T. Lopetegi, M.A.G. Laso, J. García-García, I. Gil, M. Flores Portillo, M. Sorolla, IEEE Trans. Microw. Theory Tech. **53**, 1451 (2005)
10. J. Martel, R. Marqués, F. Falcone, J.D. Baena, F. Medina, F. Martín, M. Sorolla, IEEE Microw. Wirel. Compon. Lett. **14**, 210 (2004)
11. T. Koschny, P. Markos, D.R. Smith, C.M. Soukoulis, Phys. Rev. E **68**, 656021 (2003)